

## **Comparison of Synchronous Reluctance Motors and Permanent Magnet Synchronous Motors with Direct Liquid Cooling Arrangement**

Credo Andrea, Lindh Pia, Petrov Ilya, Parasiliti Francesco, Pyrhönen Juha

This is a Final draft version of a publication  
published by IEEE  
in 2023 IEEE International Electric Machines & Drives Conference (IEMDC)

**DOI:** 10.1109/IEMDC55163.2023.10238863

### **Copyright of the original publication:**

© 2023 IEEE

### **Please cite the publication as follows:**

Credo, A., Lindh, P., Petrov, I., Parasiliti, F., Pyrhönen, J. (2023). Comparison of Synchronous Reluctance Motors and Permanent Magnet Synchronous Motors with Direct Liquid Cooling Arrangement. 2023 IEEE International Electric Machines & Drives Conference (IEMDC), San Francisco, CA, USA. DOI: 10.1109/IEMDC55163.2023.10238863

© 2023 IEEE. Personal use of this material is permitted. Permission from IEEE must be obtained for all other uses, in any current or future media, including reprinting/republishing this material for advertising or promotional purposes, creating new collective works, for resale or redistribution to servers or lists, or reuse of any copyrighted component of this work in other works.

**This is a parallel published version of an original publication.  
This version can differ from the original published article.**

# Comparison of Synchronous Reluctance Motors and Permanent Magnet Synchronous Motors with Direct Liquid Cooling Arrangement

line 1: 1<sup>st</sup> Andrea Credo  
line 2: *Department of Industrial and Information Engineering and Economics*  
line 3: *University of L'Aquila*  
line 4: L'Aquila, Italy  
line 5: andrea.credo@univaq.it

line 1: 4<sup>th</sup> Francesco Parasiliti  
line 2: *Department of Industrial and Information Engineering and Economics*  
line 3: *University of L'Aquila*  
line 4: L'Aquila, Italy  
line 5: francesco.parasiliti@univaq.it

line 1: 2<sup>nd</sup> Pia Lindh  
line 2: *LUT School of Energy Systems*  
line 3: *Lappeenranta University of Technology*  
line 4: Lappeenranta, Finland  
line 5: pia.lindh@lut.fi

line 1: 5<sup>th</sup> Juha Pyrhönen  
line 2: *LUT School of Energy Systems*  
line 3: *Lappeenranta University of Technology*  
line 4: Lappeenranta, Finland  
line 5: juha.pyrhonen@lut.fi

line 1: 3<sup>rd</sup> Ilya Petrov  
line 2: *LUT School of Energy Systems*  
line 3: *Lappeenranta University of Technology*  
line 4: Lappeenranta, Finland  
line 5: ilya.petrov@lut.fi

**Abstract**—The paper presents the comparison of Synchronous Reluctance Motors and Permanent Magnet Synchronous Motors with a Direct Liquid Cooling system. Both the solutions have been analyzed, designed, and optimized considering the same constraints in terms of geometrical encumbrance, current density, and phase voltage, for more equitable comparison. In addition, Direct Liquid Cooling introduces challenges in the selection of the number of conductors per slot and the number of slots because the slot dimensions need to satisfy an aspect ratio close to one and the adoption of a bigger conductor size. The preferred winding configuration is the concentrated one that simplifies the manufacturing process and, therefore, the cost; however, it was not possible to optimize the Synchronous Reluctance Motor with the concentrated winding arrangement achieving a competitive performance. From the comparison it is clear that mostly Permanent Magnet Synchronous Motors can exploit all the advantages of Direct Liquid Cooling, guaranteeing higher performance than Synchronous Reluctance Motors, especially in flux weakening capabilities

**Keywords**— *Direct Liquid Cooling, Electric vehicles, Optimization, Permanent Magnet Synchronous Motor, Synchronous Reluctance Motor, Thermal Design, Transportation application.*

## I. INTRODUCTION

The continuous growth in the electric vehicle market makes the companies' long-term planning more complicated for Rare Earth (RE) materials, [1]. The limited amount and market uncertainty of RE materials move the attention from the Permanent Magnet Synchronous Motors (PMSMs) (the most common solution for electric vehicles nowadays) to other candidates which do not adopt RE magnets, such as Induction Motors, Synchronous Reluctance Motors (SynRMs), and Wound Rotor Synchronous Motors, [2].

In addition, there is the aim to increase the power density of electric motors by adopting higher rotational speed, but the applicable maximum speed is also limited by the maximum mechanical stress in the rotor, which leads to an optimized

mechanical design or the adoption of new high-performance materials, [3]-[5]. Another way to increase the power density is by optimizing the thermal design, e.g. by moving the cooling system closer to the heat generation and the windings; this approach, together with applying higher rotational speed, provides a more compact motor drive configuration, [6].

It was discussed that Direct Liquid Cooling (DLC) is very promising in PMSMs, leading to a substantial increase in power density and/or reduction in temperature winding. Power density increase is crucial for weight reduction of the machine, [7]. Whereas the winding temperature reduction can improve the operating life time of the insulation and due to copper resistivity dependence on its temperature the winding operating temperature reduction is fundamental for a slight efficiency increase, which leads to a reduction in battery size and, so, a reduction in vehicle costs, [8].

In the latest papers related to the research of relatively compact motor drive systems (in the range of 1 MW), DLC is applied only to Permanent Magnet motors [9]-[10] and to Switched reluctance motors [11]-[12]; a particular case of DLC is explained and discussed in [13] in which the windings are directly cooled in a slotless motor.

In [10], the proof of concept of this cooling system has been verified and compared with the traditional indirect liquid cooling arrangement. The wires are composed of Litz wires with a steel tube inside. With DLC, it is possible to achieve higher tangential stress in the rotor, thanks to the possibility of increasing the current density in the windings, with a consequent increase of the torque and torque density of the machine. The comparison has been performed with a low-speed medium-power machine. Despite the increase of the current in the machine, the machine does not reach a high saturation level allowing to keep about constant torque current ratio up to the rated current. In addition, it is verified that DLC can strongly reduce the temperature in the windings (around 50°C of temperature reduction) compared to the traditional cooling system (indirect liquid-cooled machine) with the same output power. Also, the magnet temperature is reduced with

benefits in the torque capability and field strength of the magnet.

In [11]-[12], the DLC is applied to a Switched Reluctance Motor. Differently from the previous case, the cooling tubes are in the slot and not in the wires; therefore, the cooling capabilities of the system could be lower compared with DLC integrated into the wires. It has been demonstrated that the DLC can reduce the equivalent thermal resistance of the coils by 50% with a similar increase in power. In the maximum power operation of the DLC machine, also the losses increase by 50% with a following reduction of the efficiency (in case when the losses increase faster than the power converted by the machine). This aspect is typically verified when the DLC capability to remove the heat is used in a full extent to increase the power; however, with the same power, the reduced coil temperature (when DLC is applied) allows a reduced resistance value and a slight increase in efficiency.

In [13], a slotless motor has been considered, which presents additional challenges for cooling, such as a lower thermal mass and higher temperature rise during peak operation. To minimize these effects, the liquid cooling system replaces the winding support, which is essential for slotless motors. The main advantage of this solution is to have the cooling system closest to the windings improving the cooling capabilities. With this method, a continuous current density of 19 A/mm<sup>2</sup> and a peak current density of 39.8 A/mm<sup>2</sup> have been reached with an increase of 35% of power compared to traditional cooling systems.

However, there are no discussions about the adoption of DLC in SynRMs for torque and power density improvements, which is discussed in this paper: a comparison between a SynRM and PMSM with a DLC system has been presented, focusing on the advantages of the DLC system and evaluating if this nonstandard solution can be suitable for the SynRM to improve its power density, making it an alternative to PMSM.

The paper is organized as follows: Section II presents and describes DLC as a nonstandard thermal design for power density improvement; Section III and Section IV describe the design flow and results of the PMSM and SynRM, respectively; Section V compares and discusses the results; finally, Section VI concludes the paper.

## II. DIRECT LIQUID COOLING SYSTEM

The adopted electric motor in traction application typically uses a liquid cooling system; three different approaches are shown in Fig.1. In the traditional one, the fluid flows in the stator water jacket removing the heat (Fig.1a). This approach can be made most effective by using a moderately high number of poles – typically eight – to make stator yoke as thin as possible and therefore move the winding close to the water jacket, [14]. With the same logic the water jacket solution is mostly suitable for relatively high number of slots (to reduce single slot area) for more effective heat removal from the middle of the slot. This system is simple to manufacture but not optimal because the highest losses in electric machines are typically located in the stator windings, [15]. The heat between the stator winding and the water jacket flows through the winding insulation, the impregnation, and the stator core. Winding insulation and impregnation are manufactured with electrically insulated materials, which typically have a low thermal conductivity, making the cooling of the machine less effective.

The ideal condition is to have the liquid cooling system close to the heat generation, therefore, in the slot (Fig.1 b). This solution can also improve the cooling capability. Still, when a high number of conductors is present in the slot, the closer conductors to the water channel are well-cooled while the other ones can still reach higher temperatures and resulting in hot spots in the winding region. This aspect can be partially solved by adopting winding transposition, but good impregnation and proper sealing between the water channel and winding are needed, which limits the cooling capability of such a system [16].

The DLC system proposed in [17] presents a stainless steel tube inside the conductor. This approach somewhat reduces the copper area and, in principle, the motor efficiency (the phase resistance is getting higher), but improving the cooling capability can reduce the conductor temperature and increase the torque and the power density of the machine (Fig.1c).

This solution meets some challenges: the proposed coil (with a stainless steel tube inside) is larger than a typical coil with the same amount of copper. Therefore, the combination of the number of stator slots and the number of windings cannot be selected as freely as in general designs, but there are more constraints.

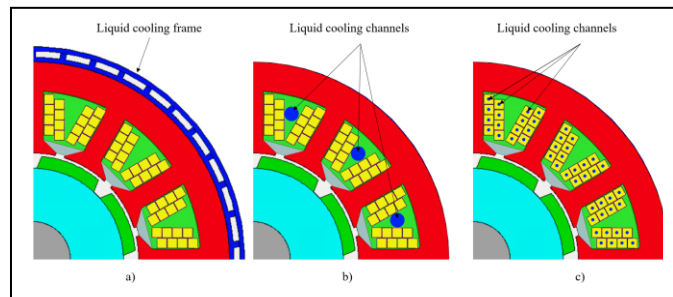


Fig. 1. Schematics of the typically adopted liquid cooling with a water jacket (a), in-slot liquid cooling (b), and the proposed direct liquid cooling (c).

Finite element analysis (FEA) was prepared to investigate the difference between PMSM operated with DLC (together with stator core cooling) and with PMSM having stator core cooling arrangement alone. Fig. 2 (a) illustrates the temperature distribution of the PMSM operating at the nominal load with DLC. The PMSM without DLC has 25% less copper losses because of a larger copper area within the winding (the space occupied by stainless tube in DLC now is occupied by copper). However, even despite smaller copper losses at the same load, the temperature rise in the winding of the PMSM without DLC is much higher than in PMSM with DLC, as shown in Fig. 2 (b). This verifies the effectiveness of the DLC. Further, in Fig. 2 (c) the temperature of the PMSM without DLC is shown in the case of 75% reduced load. Only at this load reduction, it was possible to reach the same peak temperature in the stator winding of PMSM without DLC as in the PMSM with DLC. Therefore, it can be assumed that DLC in the PMSM should allow up to 400% of extra current supply compared with the case having stator core cooling alone.

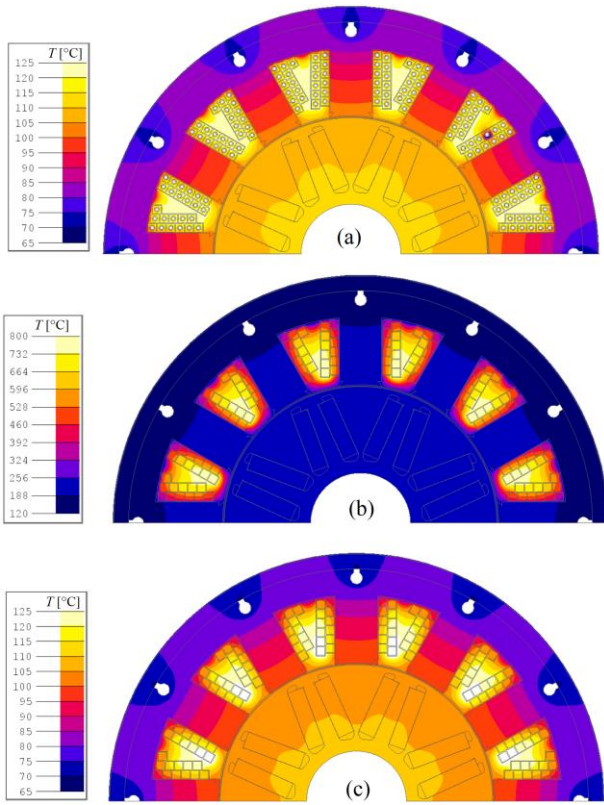


Fig. 2. Temperature distribution of the PMSM with liquid cooling, DLC at nominal load (a), with standard cooling at nominal load (b), and with standard cooling at 25% of nominal load.

Improving the cooling capabilities can strongly contribute to increase the power density, reaching very high current density, with a consequent reduction of copper area and stator slot. The reduced copper area is also a result of slightly smaller space copper factor because of the space needed for the stainless steel tube within the winding region. If the application requires a peak power for a few seconds and a lower average power during the duty cycle, as for electric car applications, it is possible to significantly increase the current density in peak conditions without having a noticeable reduction of the efficiency over the complete driving cycle. Compared to other cooling system, in this case, it is possible to maintain a low temperature inside the windings, also with a high value of current density (e.g. 10 A/mm<sup>2</sup>, the rated one for standard cooling systems), thus reducing the phase resistance, and therefore losses, guaranteeing a good efficiency.

### III. PMSM DESIGN

A 12-slot-8pole inner-rotor PMSM has been analyzed, designed, and optimized for medium-power propulsion applications. The presented design aims to validate the application of the DLC system, obtaining a motor with a high power density to be applied in the transportation sector. The slot-pole combination has been selected to have acceptable torque capability with reduced rotor losses (because the rotor does not have a separate cooling). The low number of slots allows the minimization of the electrical and hydraulic connections between the different coils, thus minimizing the manufacturing cost for the realization of the machine. In addition, the DLC needs an aspect ratio of the conductors close to one, which adds a further constraint in the optimization steps making unfeasible solutions with a high

number of conductors per slot (there is a minimum width for the conductor for the adoption of the stainless steel tube inside). This solution meets some challenges: the proposed coil (with a stainless steel tube inside) is larger than a typical coil with the same amount of copper. Therefore, the combination of the number of stator slots and the number of windings cannot be selected as freely.

The machine is designed to guarantee a rated power higher than 100 kW at 3000 rpm (325Nm), with excellent flux weakening capabilities up to 10000 rpm (the power has to be higher than 90 kW). In addition, the machine has to reach a higher torque value, 435 Nm up to 2500 rpm, for a short time. Thanks to the adopted DLC system, the current density in the rated condition can be very high compared to the other solutions, and it has been set to 19.2 A/mm<sup>2</sup>. Earlier studies [18] with DLC have shown that even 50 A/mm<sup>2</sup> is possible, but using so high values for continuous operation is often not acceptable because of too high efficiency reduction. But it can be considered as a possible power boost, at least for a short time period. Higher current densities, as well as better heat transfer, are achieved by utilizing nano liquids like CuO, Al<sub>2</sub>O<sub>3</sub>, and TiO<sub>2</sub> [25].

The main parameters of the designed machine are reported in Table I, and the sketch of the stator and rotor core together with the flux density distribution are shown in Fig. 3 and Fig. 4, respectively.

TABLE I. PMSM MAIN PARAMETERS

| Parameter                           | Unit            | Value |
|-------------------------------------|-----------------|-------|
| Stator stack iron length            | mm              | 100   |
| Stator stack iron external diameter | mm              | 306.4 |
| Stator stack air-gap diameter       | mm              | 182.4 |
| Rotor diameter                      | mm              | 180   |
| Number of stator slots              | -               | 12    |
| PM width                            | mm              | 40    |
| PM height                           | mm              | 11    |
| Stator coil-turns per phase         | -               | 48    |
| Number of conductors per slot       | -               | 12    |
| Number of pole-pairs                | -               | 4     |
| Copper wire area                    | mm <sup>2</sup> | 12    |

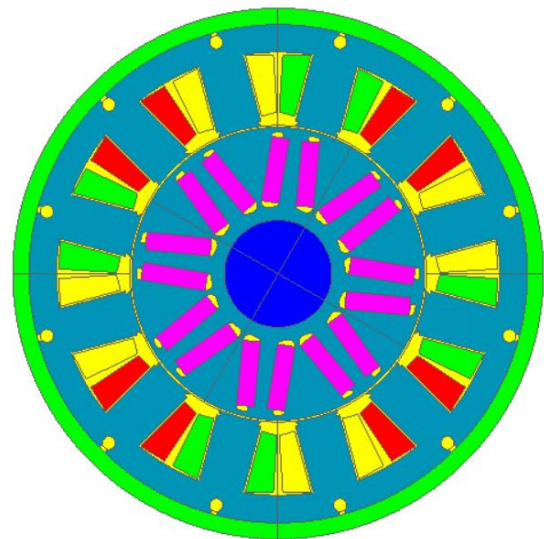


Fig. 3. Sketch of the stator and rotor core of the designed PMSM.

From the flux density, it is possible to verify the maximum level of saturation in the peak operation. A maximum value of 1.7 T is reached in the teeth and 1.6 T in the stator yoke; in these conditions, the machine works very close to the knee of the magnetization curve of the material with a slight saturation.

According to [19], it is possible to compute the pressure drop in the hydraulic circuit as a function of the desired flow rate. Considering that the coil length for each tooth is around 3.4 m and the hydraulic circuit is divided into 12 parallel paths with a total flow rate of 10 l/min, the pressure drop is 0.9 bar.

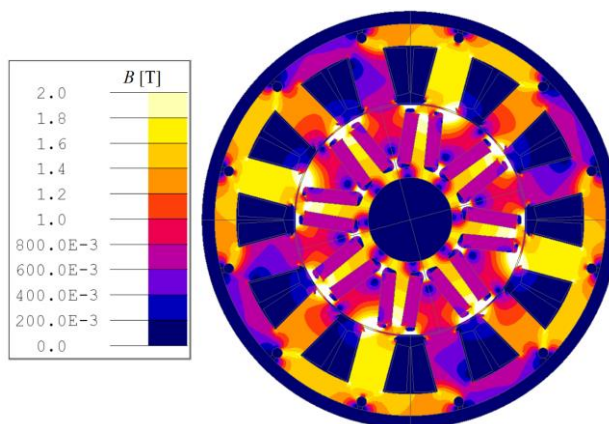


Fig. 4. Flux density distribution of the designed PMSM at the nominal load (325 Nm).

#### IV. SYNRM DESIGN

Because of the poor capabilities of SynRM with tooth-coil windings, this solution has been designed with distributed windings. The solution is more complicated from a manufacturing point of view because it needs overlapping of the coils made with the stainless steel inside. This should further increase the end-winding length of the machine compared to the classical distributed windings. However, it was verified that even larger size coils with overlapping winding can be prepared with a DLC arrangement, [20]. Therefore, the solution is still feasible, and it is worth evaluating its performance. The distributed stator windings in SynRM allow higher power and average torque with lower torque ripple than the concentrated windings. SynRM is known for its good torque per volume capability up to the base speed and good efficiency; the main limits are the relatively poor flux weakening capabilities, low power factor, and the need for structural elements inside the barrier for high-speed applications. These elements typically reduce motor performance, but they are needed from a mechanical robustness point of view.

In [4] it has been presented a solution that removes the inner ribs guaranteeing the mechanical integrity of the rotor; therefore, the design of the rotor in this paper has considered the adoption of a similar solution in order to simply compare the SynRM with the PMSM. After the comparison, mechanical analysis is fundamental for design verification. The requirements for the SynRM are the same as the PMSM, and the design flow included the choice of the best combination of the number of slots, number of poles, and number of flux barriers to satisfy them. After a preliminary evaluation of the combinations, a 54-slot-6-pole motor has been optimized with four flux barriers plus a notch. Also in

this case, the optimization is further constrained by the need for an aspect ratio of the conductors close to one, which limits the optimization. This can lead to a solution that is not fully optimized. In this case, considering the total length of the coil winding, supposing that each pole has an independent liquid cooling system, the total length of each hydraulic circuit is 6.5 m.

This means that for a total flow rate of 10 l/min, the pressure losses at 20°C are around 1 bar, which is reasonable for the application. The same current density used for the PSMS has been adopted for the design of the SynRM to maintain similar values of losses in the stator with the same cooling system. In this case, the requirements imposed by the application are not verified because of the lower power factor of this kind of machine.

It is clear that SynRM cannot reach the same performance as PM machines in terms of input current, encumbrance, maximum torque, and maximum power. For this reason, three optimizations of SynRel have been carried out:

- SynRM1 considers the same encumbrance, same maximum stator current, same base mechanical power, but different speed and torque.
- SynRM2 considers the same encumbrance, same maximum stator current, same speed, but different torque and mechanical power.
- SynRM3 considers the same maximum stator current, same speed, same torque, and mechanical power, but different encumbrance.

These three optimizations can help to understand how the SynRM can be adopted in applications in which PM motors have to be replaced for economic reasons or raw materials supply.

The maximum torque capability and the torque at the maximum speed are not inserted as constraints in the optimization, and they are only verified at the end of the optimization process. Despite the possibility of increasing the encumbrance of the motor, the poor flux weakening capabilities and the high saturation required for these levels of power strongly affect these two operating points, making the optimization unfeasible.

Table II shows the main parameters geometrical and winding of the three optimized SynRM, while their performance is reported and discussed in the next Section.

TABLE II. SYNRM MAIN PARAMETERS

| <i>Parameter</i>                    | <i>Unit</i>     | <i>SynRM 1</i> | <i>SynRM 2</i> | <i>SynRM 3</i> |
|-------------------------------------|-----------------|----------------|----------------|----------------|
| Stator stack iron length            | mm              | 100            | 100            | 110            |
| Stator stack iron external diameter | mm              | 306.4          | 306.4          | 330.0          |
| Stator stack air-gap diameter       | mm              | 196.3          | 181.3          | 205.0          |
| Rotor diameter                      | mm              | 195.3          | 180.3          | 204.0          |
| Number of stator slots              | -               | 54             | 54             | 54             |
| Tooth width                         | mm              | 6.4            | 6.2            | 6.9            |
| Conductor width                     | mm              | 5.5            | 5.5            | 5.5            |
| Stator coil-turns per phase         | -               | 36             | 45             | 45             |
| Number of conductors per slot       | -               | 4              | 5              | 5              |
| Number of pole-pairs                | -               | 3              | 3              | 4              |
| Copper wire area                    | mm <sup>2</sup> | 14.0           | 14.0           | 14.0           |

The cross section of the three optimized solution is quite similar and for lack of clarity only the one of SynRM1 is presented in Fig. 5, while the flux density in the peak operation is shown in Fig. 6.

The figure shows a very high level of saturation; stator teeth and yoke reach 1.8 T with a string reduction of the saliency ratio and, therefore, of the performance.

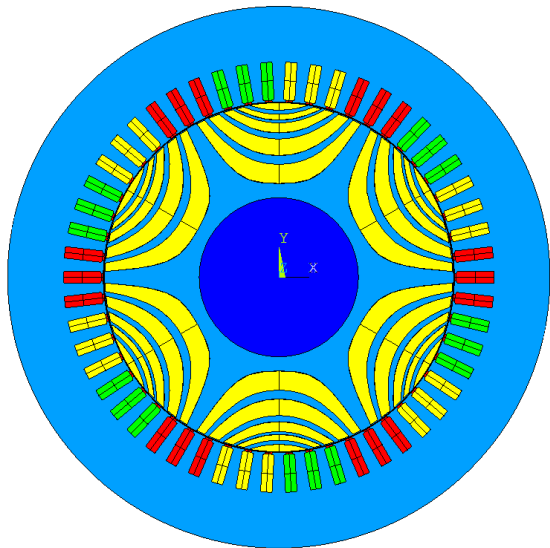


Fig. 5. Sketch of the stator and rotor core of the designed SynRM.

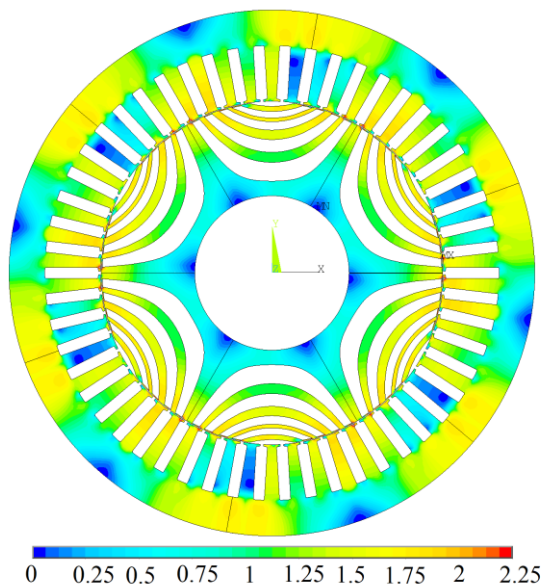


Fig. 6. Flux density map (T) at maximum torque operation.

## V. COMPARISON

The results of the PMSM and the three optimized SynRM solutions have been compared, and the performances are shown in Table III. In the table in bold there are the parameters or performance which are equal compared to the PMSM design. The same constraints of all optimizations are current density and phase voltage. Because of the lower power factor of the SynRM than PMSM, it is impossible to reach the same performance, with the same encumbrance and speed, in terms of base power. However, the optimized design of SynRMs shows other important features of this kind of machine.

The PMSM is able to reach very high rated torque and power density (34.46 Nm/l and 10.6 kW/l) and the high short time torque density (46.1 Nm/l and 12.1 kW/l). Also, the constraint in terms of flux weakening is fully satisfied with a torque at the maximum speed of 10000 rpm equal to 95 Nm and a power of 99 kW. Differently, SynRM designs are not able to satisfy all the constraints also with a moderate increase of the encumbrance.

TABLE III. PERFORMANCE COMPARISON

| Parameter                          | Unit              | PMSM         | SynRM 1      | SynRM 2      | SynRM 3      |
|------------------------------------|-------------------|--------------|--------------|--------------|--------------|
| <b>Geometrical parameters</b>      |                   |              |              |              |              |
| External diameter                  | mm                | <b>306.4</b> | <b>306.4</b> | <b>306.4</b> | 330.0        |
| Stator iron length                 | mm                | <b>100</b>   | <b>100</b>   | <b>100</b>   | 110          |
| <b>Rated operation @base speed</b> |                   |              |              |              |              |
| Base speed                         | rpm               | <b>3000</b>  | 4500         | <b>3000</b>  | <b>3000</b>  |
| Base frequency                     | Hz                | 200          | 275          | 150          | 150          |
| Base torque                        | Nm                | <b>325</b>   | 211          | 260          | <b>320</b>   |
| Base mech. power                   | kW                | <b>102</b>   | <b>99</b>    | 82           | <b>100</b>   |
| Base stator current                | A                 | 230          | 270          | 270          | 248          |
| Current angle control              | deg               | 43           | 65           | 67           | 61           |
| Power factor                       |                   | 0.75         | 0.66         | 0.61         | 0.70         |
| Efficiency                         | %                 | 93.8         | 93.0         | 91.7         | 92.4         |
| Current density                    | A/mm <sup>2</sup> | 19.2         | 19.2         | 19.2         | 17.6         |
| <b>Peak torque operation</b>       |                   |              |              |              |              |
| Maximum torque                     | Nm                | <b>435</b>   | 260          | 320          | 415          |
| Max. mech. Power                   | kW                | 114          | 100          | 89           | 109          |
| Speed at max. power                | rpm               | <b>2500</b>  | 3700         | 2700         | <b>2500</b>  |
| Max. stator current                | Arms              | <b>350</b>   | <b>350</b>   | <b>350</b>   | <b>350</b>   |
| Current angle control              | deg               | 53           | 72           | 76           | 70           |
| Power factor                       |                   | 0.59         | 0.50         | 0.48         | 0.54         |
| Efficiency                         | %                 | 89.2         | 89.6         | 88.5         | 89.3         |
| Current density                    | A/mm <sup>2</sup> | 29.2         | 29.2         | 29.2         | 29.2         |
| <b>Maximum speed operation</b>     |                   |              |              |              |              |
| Torque at max. speed               | Nm                | 94           | 34           | 38           | 69           |
| Power at max. speed                | kW                | 98           | 48           | 40           | 72           |
| Maximum speed                      | rpm               | <b>10000</b> | 13500        | <b>10000</b> | <b>10000</b> |

The base performance for SynRMs has been reached for SynRM1 and SynRM3 with a slight increase of the phase current (+17% for SynRM1 and +8% for SynRM3). Despite the same increase in the base current of SynRM3, the motor was not able to reach the same mechanical power. The increase in the current is followed by a slight increase in the copper wire area (in order to maintain the same current density for thermal issues) and an increase in the slot area.

Focusing the considerations on SynRM1, only the base mechanical power and the encumbrance are satisfied, while there is an increase in the base and the maximum speed of 50%. The maximum torque is reduced by 40% and, considering the different speed and the different gear ratio to be used in the application, there is a lower wheel torque (around 10%). However, also the power at the maximum

speed is not satisfied with a reduction compared to the PMSM design by 50%.

SynRM2 only satisfies the constraints in terms of encumbrance and base speed, but there is a reduction in torque (20%), mechanical power (20%), maximum torque (22%), maximum mechanical power (22%), and power at maximum speed (60%).

SynRM3 satisfies the base torque and speed and maximum torque and power with a slight increase of encumbrance (around 30% in volume). Despite the increase of the volume, the solution does not reach the performance of the PSMS in terms of maximum power and torque at the maximum speed with a reduction of 26%.

Another negative aspect of SynRM solutions is the need to adopt distributed windings that have longer end windings; therefore, it is necessary to use a lower number of conductors per phase in order to maintain similar values of phase resistance and Joule losses. There is also a slight reduction of efficiency both in the base point and in the maximum power one because the motors have similar values of losses with different values of output power. In addition to what was discussed, the SynRM has a further limitation, the most important one is the poor flux weakening capability because the motor peak torque is strongly limiting the performance in the field weakening. This aspect could be critical in the function of the application.

From this detailed comparison between SynRMs and PMSM it is clear that the first one cannot reach the same performance of the second, but with a slight increase of speed and encumbrance, it is possible to have comparable solutions. The main advantage of the DLC is the possibility to strongly increase the maximum current density in the windings with a consequent increase of the peak operating performance. This can be verified in the SynRM thanks to the higher steel area, which allow the machine to work with lower saturation condition in the base operation, thus having a little margin for peak power operation.

The choice between SynRM and PSMS should be investigated in terms of cost, raw materials, and performance constraints. If the application admits a slight increase in speed and encumbrance, modifying the transmission system, SynRM can be used to replace PMSM. However, a system cost investigation is necessary in order to evaluate how the reduction of efficiency and power factor of SynRMs increase the costs of the power electronics and battery size in order to guarantee the same kilometers range.

## VI. CONCLUSION

This paper presents the adoption of a nonstandard DLC system to enhance electric cars' power and torque density for automotive applications. The cooling of the machine close to the heat generation (windings) can strongly enhance the base power of the machine with the same geometrical constraints. In order to verify this, two motor solutions have been analyzed, designed, and optimized. The PMSM adopted in this study uses concentrated windings to reduce the end-windings length and simplify the manufacturing of the machine and the cooling system. The SynRM designed in this study uses distributed windings in order to maximize the performance of the machine accepting a more complicated manufacturing step. However, despite the adoption of a more complicated winding structure. The SynRM is not able to

reach the performance of PMSM in terms of base power, efficiency, and flux weakening capability. The limits of SynRM were well known if compared to PMSM, but in some cases, they can be partially compensated with the adoption of a bigger encumbrance, higher phase current, and higher base speed. These limitations are enhanced with the DLC mainly due to the poor flux weakening capabilities; the high power density can be reached with a high saturation level of the machine, which further affects the flux weakening capabilities of the machine. In addition, the higher costs of the windings do not justify their adoption in SynRMs.

## REFERENCES

- [1] "Materials: a potential bottleneck to deployment of low-carbon technologies in the EU? - EU Science Hub - European Commission", EU Science Hub - European Commission, 2021. [Online]. Available: <https://ec.europa.eu/jrc/en/news/materials-potential-bottleneck-deployment-low-carbon-technologies-eu>.
- [2] A. Credo, M. Villani, G. Fabri and M. Popescu, "Adoption of the Synchronous Reluctance Motor in Electric Vehicles: a Focus on the Flux Weakening Capability," in *IEEE Transactions on Transportation Electrification*, 2022.
- [3] M. Di Nardo et al., "High-Speed Synchronous Reluctance Machines: Materials Selection and Performance Boundaries," in *IEEE Transactions on Transportation Electrification*, vol. 8, no. 1, pp. 1228-1241, March 2022.
- [4] A. Credo, M. Villani, M. Popescu and N. Riviere, "Application of Epoxy Resin in Synchronous Reluctance Motors With Fluid-Shaped Barriers for E-Mobility," in *IEEE Transactions on Industry Applications*, vol. 57, no. 6, pp. 6440-6452, Nov.-Dec. 2021.
- [5] C. Babetto, G. Bacco and N. Bianchi, "Synchronous Reluctance Machine Optimization for High-Speed Applications," in *IEEE Transactions on Energy Conversion*, vol. 33, no. 3, pp. 1266-1273, Sept. 2018.
- [6] A. Acquaviva, S. Skoog and T. Thiringer, "Design and Verification of In-Slot Oil-Cooled Tooth Coil Winding PM Machine for Traction Application," in *IEEE Transactions on Industrial Electronics*, vol. 68, no. 5, pp. 3719-3727, May 2021.
- [7] S. Schlimpert et al., "Experimental & Modelling Study of Advanced Direct Coil Cooling Methods in a Switched Reluctance Motor," 2020 *IEEE Vehicle Power and Propulsion Conference (VPPC)*, Gijon, Spain, 2020, pp. 1-5.
- [8] A. Babin, N. Rizoug, T. Mesbahi, D. Boscher, Z. Hamdoun and C. Larouci, "Total Cost of Ownership Improvement of Commercial Electric Vehicles Using Battery Sizing and Intelligent Charge Method," in *IEEE Transactions on Industry Applications*, vol. 54, no. 2, pp. 1691-1700, March-April 2018.
- [9] P. Lindh, I. Petrov, J. Pyrhönen, E. Scherman, M. Niemelä and P. Immonen, "Direct Liquid Cooling Method Verified With a Permanent-Magnet Traction Motor in a Bus," in *IEEE Transactions on Industry Applications*, vol. 55, no. 4, pp. 4183-4191, July-Aug. 2019.
- [10] P. M. Lindh et al., "Direct Liquid Cooling in Low-Power Electrical Machines: Proof-of-Concept," in *IEEE Transactions on Energy Conversion*, vol. 31, no. 4, pp. 1257-1266, Dec. 2016.
- [11] J. Nonneman, S. Schlimpert, I. T'Jollyn and M. D. Paepe, "Modelling and Validation of a Switched Reluctance Motor Stator Tooth with Direct Coil Cooling," 2020 *19th IEEE Intersociety Conference on Thermal and Thermomechanical Phenomena in Electronic Systems (ITherm)*, Orlando, FL, USA, 2020.
- [12] . Schlimpert et al., "Experimental & Modelling Study of Advanced Direct Coil Cooling Methods in a Switched Reluctance Motor," 2020 *IEEE Vehicle Power and Propulsion Conference (VPPC)*, Gijon, Spain, 2020, pp. 1-5.
- [13] R. Chattopadhyay, M. S. Islam, J. Jung, R. Mikail and I. Husain, "Winding Embedded Liquid Cooling for Slotless Motors in Transportation Applications," in *IEEE Transactions on Industry Applications*, vol. 58, no. 6, pp. 7110-7120, Nov.-Dec. 2022.
- [14] D. P. Kulkarni, G. Rupertus and E. Chen, "Experimental Investigation of Contact Resistance for Water Cooled Jacket for Electric Motors and Generators," in *IEEE Transactions on Energy Conversion*, vol. 27, no. 1, pp. 204-210, March 2012.

- [15] S. Wu, D. Hao and W. Tong, "Cooling System Design and Thermal Analysis of Modular Stator Hybrid Excitation Synchronous Motor," in *CES Transactions on Electrical Machines and Systems*, vol. 6, no. 3, pp. 241-251, September 2022.
- [16] W. Geng, T. Zhu, Q. Li and Z. Zhang, "Windings Indirect Liquid Cooling Method for a Compact Outer-Rotor PM Starter/Generator With Concentrated Windings," in *IEEE Transactions on Energy Conversion*, vol. 36, no. 4, pp. 3282-3293, Dec. 2021.
- [17] I. Petrov, P. Lindh, M. Niemelä, E. Scherman, O. Wallmark and J. Pyrhönen, "Investigation of a Direct Liquid Cooling System in a Permanent Magnet Synchronous Machine," in *IEEE Transactions on Energy Conversion*, vol. 35, no. 2, pp. 808-817, June 2020.
- [18] C. Di, I. Petrov and J. Pyrhönen, "Estimation of Continuous Power of a Permanent Magnet Synchronous Machine Equipped with Direct-Liquid-Cooling Winding for Propulsion Applications by EFA," 2020 International Conference on Electrical Machines (ICEM), Gothenburg, Sweden, 2020, pp. 854-859.
- [19] P. Lindh et al., "Performance of a Direct-Liquid-Cooled Motor in an Electric Bus Under Different Load Cycles," in *IEEE Access*, pp. 86897-86905, 2019.
- [20] E. Kurvinen *et al.*, "Design and Manufacturing of a Modular Low-Voltage Multimegawatt High-Speed Solid-Rotor Induction Motor," in *IEEE Transactions on Industry*
- [21] G. Saxena and P. Soni, "Nano Coolants for Automotive Applications: A Review," *Nano Trends: A Journal of Nanotechnology and Its Applications*, vol. 20, no. 1, pp. 9-22, 2018.